

The partial widths of the 16.1 MeV 2^+ resonance in ^{12}C

Michael Munch¹ and Hans Otto Uldall Fynbo¹

Department of Physics and Astronomy, Aarhus University, Ny Munkegade 120, 8000 Aarhus C, Denmark

Received: date / Revised version: date

Abstract. The 16.1 MeV 2^+ resonance in ^{12}C situated slightly above the proton threshold can decay by proton-, α -, and γ emission. The partial width for proton emission cannot be directly measured due to the low proton energy and the small branching ratio. Instead it must be indirectly derived from other observables. However, due to several inconsistent data the derived partial width varies by almost a factor 2 dependent on the data used. Here we trace the majority of this inconsistency to different measurements of the (p, α) cross sections. We have remeasured this cross section using modern large area silicon strip detectors allowing to measure all final state particles, which circumvents a normalization issue affecting some of the previous measurements. Based on this we determine $\Gamma_p = 21.0(13)$ eV. We discuss the implications for other observables related to the 16.1 MeV 2^+ resonance.

PACS. 23.20.+e α decay – 27.20.+n Properties of specific nuclei listed by mass ranges; $6 \leq A \leq 19$

1 Introduction

Situated just above the proton threshold the 16.1 MeV 2^+ state in ^{12}C has been the subject of numerous studies [1, 2, 3, 4, 8, 9, 5, 6, 10, 11, 7, 12, 13] with the most recent review published in Ref. [14] and a detailed review of the 16.1 MeV state given in [12]. The state has primarily been investigated with the $p + ^{11}\text{B}$ reaction and it is known to decay via proton, α particle and γ ray emission as illustrated in Figure 1. In the narrow resonance limit the measured cross sections, σ_{px} , can be related to the partial widths, Γ_x , of the resonance

$$\sigma_{px} = 4\pi\lambda^2\omega \frac{\Gamma_p\Gamma_x}{\Gamma^2}. \quad (1)$$

Γ_p has a key role in this relation, but due to the low proton energy and the fact that $\Gamma_p/\Gamma \ll 1$, it is not feasible to measure it directly. Instead, Γ_p must be inferred from measurements of both Γ_x and σ_{px} . This extraction was performed in both review articles, however, the resulting proton widths differ by almost a factor of 2 [12, 14]. This strongly impacts the expected yield from the $p + ^{11}\text{B}$ reaction, which has long been a prime candidate for use in a aneutronic fusion reactor [15]. In the following we will summarize the results of previous measurements and attempt clarify the situation.

γ ray emission predominantly occur to the ground state (GS), γ_0 , and the first excited state, γ_1 , in ^{12}C . The cross sections for the (p, γ) reactions were most recently measured by [13] using a thin target for the first time [13].

Here they confirmed the prior cross section measurements [1, 16, 17, 10, 18, 4, 8] yielding a combined result of $\sigma_{p\gamma 0} = 5.1(5)$ μb and $\sigma_{p\gamma 1} = 139(12)$ μb . Thus we consider the values for these cross sections to be reliable. Complementary to these measurements, [9] directly measured $\Gamma_{\gamma 0} = 0.346(41)$ eV using inelastically scattered electrons [9], while [10] have measured the relative yield of γ rays and charged particles; $\Gamma_{\gamma 0}/\Gamma_{\alpha} = 6.7(3) \times 10^{-5}$ and $\Gamma_{\gamma 1}/\Gamma_{\alpha} = 2.0(3) \times 10^{-3}$.

The current understanding of the α particle decay mechanism is a sequential decay proceeding either through the ^8Be GS, α_0 , or the first excited state, α_1 [7]. The results of prior investigations of the (p, α) channel are listed in Table 1. There are multiple consistent measurements for the

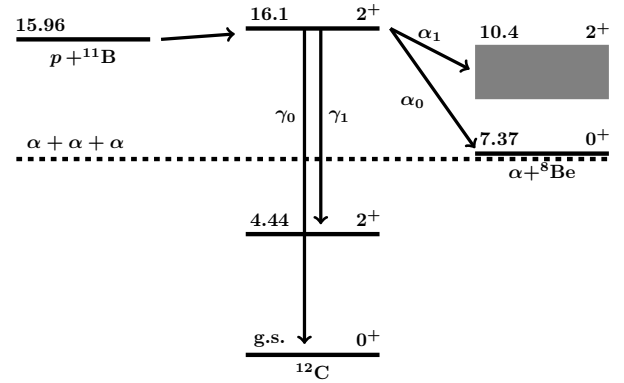


Fig. 1. Illustration of the reaction scheme. The 16.11 MeV 2^+ state ^{12}C is populated with the $p + ^{11}\text{B}$ reaction. The state can either decay via γ , α or proton emission. Energies and spin assignments are taken from Ref. [14]. Energies are in MeV.

Send offprint requests to: Hans Fynbo

Table 1. Prior measurements of the (p, α) channel.

Measurement	$\sigma_{\alpha,0}$ [mb]	$\sigma_{\alpha,1}$ [mb]	σ_{α} [mb]	$\sigma_{\alpha,1}/\sigma_{\alpha,0}$	Γ [keV]
Huus <i>et al.</i> [1]					~ 5
Beckman <i>et al.</i> [2]	$0.2 \pm 30\%$ ¹	$10 \pm 30\%$ ¹			
Segel <i>et al.</i> [3]				22(3)	
Anderson <i>et al.</i> [4]			41(3) ²		6.7
Davidson <i>et al.</i> [5]			54(6)		$5.2^{+0.5}_{-0.3}$
Becker <i>et al.</i> [6]	$2.12 \pm 5\%$	$69.6 \pm 5\%$ ³		33(2)	5.3(2)
Laursen <i>et al.</i> [7]				19.6(19)	

¹ The authors note that the α particles were “barely detectable” [2]. This result will be disregarded.

² Assuming infinite target thickness and using the combined Γ of Ref. [6,4] this should be rescaled from 38.5(32) mb.

³ The authors note that their model did *not* reproduce the α_1 data.

resonance width and combining the results from Refs. [5, 6] yield 5.28(18) keV. As these are extracted from a simple resonance scan we consider them reliable. Two out of three measurements of the α_1/α_0 branching ratio are consistent and, as the measurement by [7] was done with coincident detection of multiple final state particles, we also consider the branching ratio reliable. The measured total cross sections for (p, α) generally show poor agreement. However, considering the (p, α_0) reaction yields a distinct high energy peak we expect the σ_{p,α_0} measurement by [6] to be accurate.

By combining the various measurements for the α - and γ channels with Eq. (1) and approximating $\Gamma \approx \Gamma_{\alpha}$ it is possible to derive several independent values for Γ_p . These are listed in Table 2. Interestingly, the values seem to cluster into two groups, with the measurements for (p, α) split across the groups.

All of the cross section measurements of the (p, α) channel were performed with a small energy sensitive detector placed at various angles. The measured energy spectrum was then extrapolated to 0 and integrated. Refs. [5, 4] performed a linear extrapolation, while Ref. [6] used a sequential decay model. Although [6] note their model performed poorly at this resonance, it does *not* explain the discrepancy between the measurements. The key difference is the choice of normalization for the α_1 measurement where [6] argue that their detector have either detected the primary alpha particle α_1 or the two secondary α particles from the subsequent ^8Be break-up. Thus, they

divide their counter number by 2. On the contrary, Refs. [5,4] argue they observe one out three final state α particles. They divide by a factor of 3. The probability for detecting both secondary α particles in a single detector was discussed theoretically by Wheeler in 1941 [19]. The probability depends on the opening angle between the secondary α particles and the aperture of the detector. The opening angle in turn depends on the energy of the ^8Be system with respect to the α threshold. This is small for the GS but quite significant for the first excited state. Based on information provided in Ref. [6] we have estimated their maximum detector aperture to be of the order of 3° . In this case the probability for a double hit is minuscule - even for the α_0 channel. Thus, the α_1 results by [6] should most likely be scaled by a factor of 2/3 making it consistent with the other two measurements.

The object of this paper is to remeasure $\sigma_{p\alpha}$ in order to test the above statement. The measurement will circumvent the normalization ambiguity by observing all three particles in coincidence using an array of large area segmented silicon detectors. In this paper we will only address the cross section of the 16.1 MeV state, but the discussion on normalization applies universally to all measurements of this reaction, where the cross section is inferred from a single detector.

2 Experiment

A thin foil of ^{11}B , oriented 45° with respect to the beam axis, was bombarded with a beam of H_3^+ molecules. A resonance scan was conducted between 460 and 600 keV and afterwards data was collected for 30 hours at 525 keV. The beam was provided by the 5 MV Van de Graaff accelerator at Aarhus University and the beam spot was defined by a pair of 1×1 mm vertical and horizontal slits. The energy of the accelerator was prior to the experiment energy calibrated using narrow resonances (p, α) in ^{27}Al and the energy resolution was found to be better than a few keV for single charged beams. It should be noted that the energy stability is trifold improved for H_3^+ .

Upon impact with the target foil the H_3^+ molecules will break up and additional electron stripping, neutralization and scattering might occur. This affected the integrated beam current, which was measured with a Faraday

Table 2. Calculated values for Γ_p . The values are calculated using Eq. (1) with the quantities listed in the left column. In all cases $\Gamma = 5.28(18)$ keV was also used. The approximation $\Gamma_{\alpha} \approx \Gamma$ was applied.

Method	Γ_p [eV]
$\sigma_{p\alpha}$ [4]	20(2)
$\sigma_{p\alpha_0}$ [6] + $\Gamma_{\alpha_1}/\Gamma_{\alpha_0}$ [3,7]	22(3)
$\sigma_{p\alpha}$ [5]	26(3)
$\sigma_{p\alpha}$ [6]	34(6)
$\sigma_{p\gamma_1}$ [13] + $\Gamma_{\gamma_1}/\Gamma_{\alpha}$ [10]	35(3)
$\sigma_{p\gamma_0}$ [13] + $\Gamma_{\gamma_0}/\Gamma_{\alpha}$ [10]	37(6)
$\sigma_{p\gamma_0}$ [13] + Γ_{γ_0} [9]	38(6)

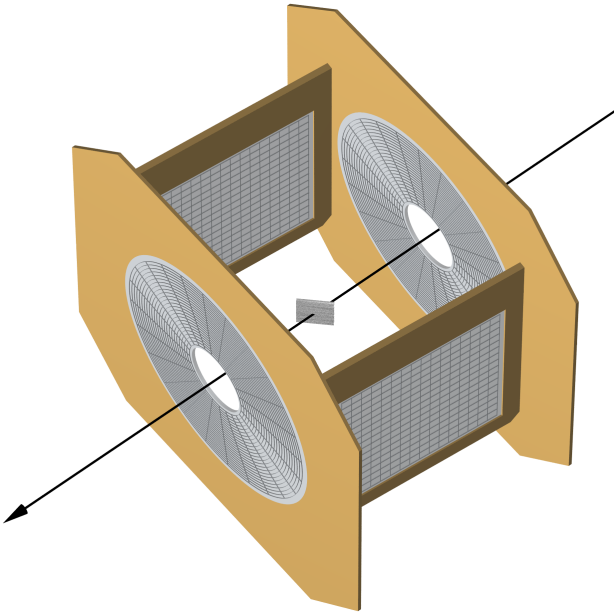


Fig. 2. Schematic drawing of the experimental setup. An arrow indicates the incoming proton beam. The enriched boron target was oriented 45° with respect to the beam axis. Two quadratic and two annular double sided silicon strip detector were used to detect outgoing particles. Front and back segmentation is shown simultaneously for clarity.

cup 1 m downstream of the target. The combined effect of this can be determined from the ratio of the observed current both with and without a target foil in the beam. At the beginning of the experiment the effective charge state was determined to be $1.72(5)e$. However, this ratio was observed to change during the experiment. We attribute this to carbon build-up on the target. The change in charge state was $4.33(4) \times 10^{-3} \mu\text{C}^{-1}$. Correcting for this, a total of $61(6) \mu\text{C}$ was collected on the resonance.

The target was produced at Aarhus University by evaporation of 99% enriched ^{11}B onto a $4 \mu\text{g}/\text{cm}^2$ carbon backing. The thickness was measured by bombarding the target with 2 MeV α particles and the boron layer either facing towards or away from the beam. Assuming a two layer target the boron thickness can be inferred from the energy shift of particles scattered off the carbon layer using the procedure of Ref. [20], but including a correction for the changed stopping power of the scattered particle.

$$t = \frac{\delta E}{K(\theta)S(E_b) + S(K(\theta)E_b)/\cos\theta}, \quad (2)$$

where K is the kinematic factor evaluated for the scattering angle θ , E_b the beam energy, S the stopping power and δE the energy difference. The cosine factor corrects for the increased path length for the scattered particle. The result is $39(3) \mu\text{g}/\text{cm}^2$. The energy loss for a $525/3 \text{ keV}$ proton through this target is $23(2) \text{ keV}$ according to the SRIM stopping power tables of [21] [21].

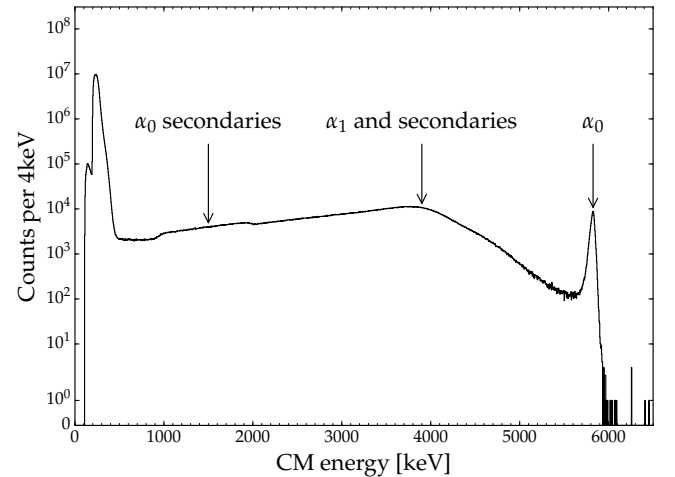


Fig. 3. Full CM energy spectrum without any cuts. The high energy peak corresponds to the primary α particle, α_0 .

Charged particles were observed with an array of double sided silicon strip detectors (DSSD) giving a simultaneous measurement of position and energy. A sketch of the array can be seen on Figure 2. The array consisted of two annular DSSD (S3 from Micron Semiconductors) placed 36 mm up- and downstream of the target; covering the angles between 140 and 165° and 23 and 36° respectively. Additionally, two quadratic DSSDs (W1 from Micron Semiconductors) were placed 40 mm from the target center at an angle of 90° with respect to the beam axis. These covered angles between 60° and 120° .

3 Analysis

The analysis is structured in the following way. First a resonance scan is shown for the α_0 channel. This is followed by an extraction of the α_0 angular distribution and cross section from the multiplicity 1 data. Building upon this follows the analysis of the triple events i.e. events with exactly three alpha particles and afterwards a brief discussion of how the detection efficiencies for the α_0 and α_1 channel have been determined.

3.1 Singles analysis

Assuming all ejectiles to be α particles the center-of-mass (CM) energy can be determined from the detected position and energy. The full spectrum, without any cuts, is shown in Figure 3. The spectrum shows a clear peak at 5.8 MeV , which is consistent with a sequential decay of the 16.1 MeV state via the GS of ^8Be . The α particle giving rise to this peak will be referred to as the primary α particle. Below the peak is a broad asymmetric distribution, which consists of secondary α particles and α particles from the break-up via the first excited state of ^8Be . At low energy the proton peak is visible. It is double peaked

since energy loss corrections are applied as if it was an α particle.

The primary α particle is selected by requiring $E_{\text{CM}} > 5.65$ MeV. Figure 4 shows the α_0 yield as a function of proton energy. The yield is clearly resonant and peaks at ~ 175 keV. The curve shown in the figure is the best fit to

$$Y = \left[\tan^{-1} \frac{E_p - E_r}{\Gamma_{\text{lab}}/2} - \tan^{-1} \frac{E_p - E_r - \Delta E}{\Gamma_{\text{lab}}/2} \right] \times \frac{\Gamma_{\text{lab}} \sigma_{\text{BW}}(E = E_r)}{2\epsilon} \eta, \quad (3)$$

where Γ_{lab} is the resonance width in the lab system, E_p is the beam energy, E_r the resonance energy, ΔE the energy loss through the target, η the detection efficiency, σ_{BW} the resonant Breit-Wigner cross section and $\epsilon = \frac{1}{N} \frac{dE}{dx}$, where N is the number density of target nuclei and $\frac{dE}{dx}$ the stopping power. Using the factor outside the parenthesis as an arbitrary scaling factor, the best fit was achieved with $\Delta E = 24.5(9)$ keV, $E_r = 162.6(5)$ keV and Γ_{lab} fixed to $12/11 \cdot 5.28$ keV. The target thickness is consistent with the result obtained from α -scattering and the resonance energy fits with the recommended literature value [18].

The α_0 angular distribution relative to the beam axis was extracted for the long runs at $E_p = 175$ keV. The angular distribution, corrected for solid angle, can be seen in Figure 5. The solid line shows the best fit to the lowest five Legendre polynomials.

$$W(\theta) = A \left[1 + \sum_{i=1}^4 a_i P_i(\cos \theta) \right]. \quad (4)$$

The coefficients providing the best fit are $a_1 = -0.358(7)$, $a_2 = 0.249(2)$, $a_3 = -0.106(11)$, $a_4 = -9(20) \times 10^{-3}$ and $A = 4.253(17) \times 10^4 \text{ sr}^{-1}$. The lower panel of the figure shows the fit rescaled, $W(90^\circ) = 1$, along with the data

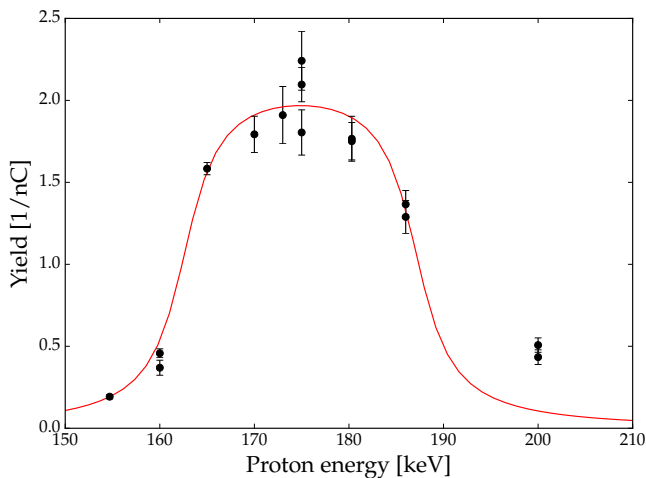


Fig. 4. Scan of the 162 keV resonance. The individual data points corresponds to the α_0 yield, while the solid curve is the best fit to Eq. (3).

from Refs. [6,5], which have been rescaled to coincide with the fit at 90° .

The total number of counts is found by integration of Eq. (4) i.e. $4\pi A$. This can be related to the resonant Breit-Wigner cross section using Eq. (3)

$$\sigma_{p\alpha,0} = 2.1(2) \text{ mb}. \quad (5)$$

The main uncertainty is the variation in the effective charge state.

3.2 Extraction of triple events

The end goal of this analysis step is to extract tuples of particles consistent with a decay of the 16.1 MeV state in ^{12}C into three α particles. It applies the methods described in Ref. [22].

The first and simplest requirement is that at least three particles must be detected in an event. This massively reduces the data, since the majority of events consist of elastically scattered protons. Furthermore, it is required that all three particles are detected within 30 ns of each other. This reduces the background from random coincidences with protons significantly while $> 99\%$ of good events survive. Additionally, it is required that the sum of CM angles between the CM position vectors must be larger than 350° . All particles surviving these cuts are assumed to be α particles. From the detected energy and position it is possible to calculate the four momentum of each particle. From these, one can calculate the total momentum in the CM and the ^{12}C excitation energy. This is shown in Figure 6, which has a distinct peak at 16.1 MeV. Interestingly, weak peaks are visible at low total momentum and excitation energy lower than 16.1 MeV. These correspond to γ transitions in ^{12}C as observed in Ref. [12]. Projecting the individual energy of the high momentum events it is clear that these correspond to events with one proton and

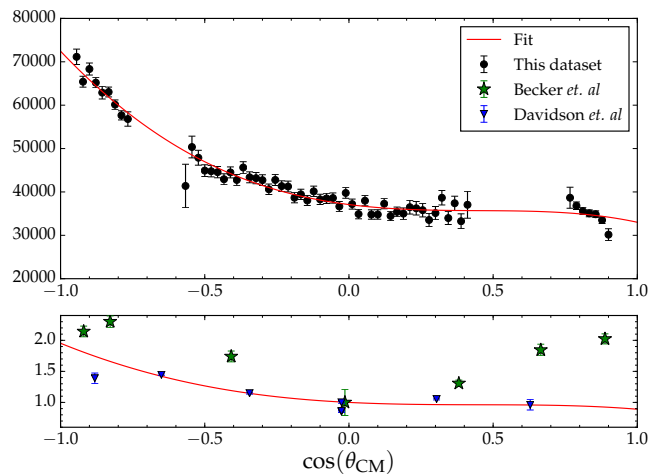


Fig. 5. Angular distribution of this dataset corrected for solid angle along with the best fit to Eq. (4). The datasets of Ref. [6,5] have been rescaled to coincide with the fit at 90° .

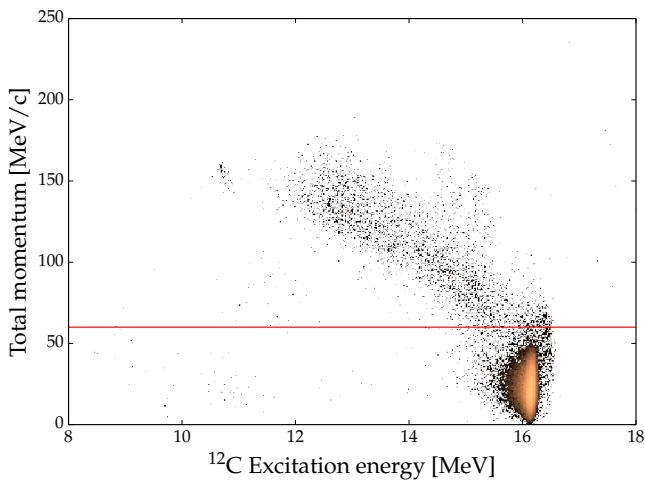


Fig. 6. Total momentum of the three particles in the CM vs. the calculated excitation energy of ^{12}C . The red line corresponds to the cut placed at 60 MeV/c.

two α particles. Hence, all events with $p_{\text{CM}} > 60$ MeV/c are removed.

In order to classify whether a tuple corresponds to a decay via the GS or first excited state, it is convenient to make a Dalitz plot with coordinates defined as

$$x = \frac{\epsilon_1 + 2\epsilon_2 - 1}{\sqrt{3}} \quad y = \epsilon_1 - 1/3, \quad (6)$$

where $\epsilon_i = E_i^{\text{CM}}/E_{\text{tot}}$. The Dalitz plot can be seen in Figure 7, where a choice of ordering has been made, so index 1 corresponds to the lowest energy. The circle corresponds to the limits imposed by energy and momentum conservation. The dashed red line corresponds to a low energy cutoff imposed by thresholds in the analysis and data acquisition hardware. The peak in the lower right corner corresponds to one α particle having maximum energy i.e. a decay via the ^8Be GS. This exceeds the conservation limit due to non-perfect energy loss corrections and pixelation effects. The dotted green line indicates the classification into either a decay via the GS (right) or the first excited state (left) and is equivalent to the cut applied in Section 3.1. This Dalitz plot was studied extensively in Ref. [7]. The observed number of counts is then calculated by integration of these areas

$$N_0 = 3.318(18) \times 10^4 \quad (7)$$

$$N_1 = 4.33(2) \times 10^4, \quad (8)$$

where the uncertainties are due to counting statistics.

3.3 Detection efficiency of the α_0 channel

In order to relate the observed number of counts to a yield it is necessary to determine the detection efficiency. For the ground state this is simple. A beam with a 1×1 mm profile was generated and propagated to a random depth

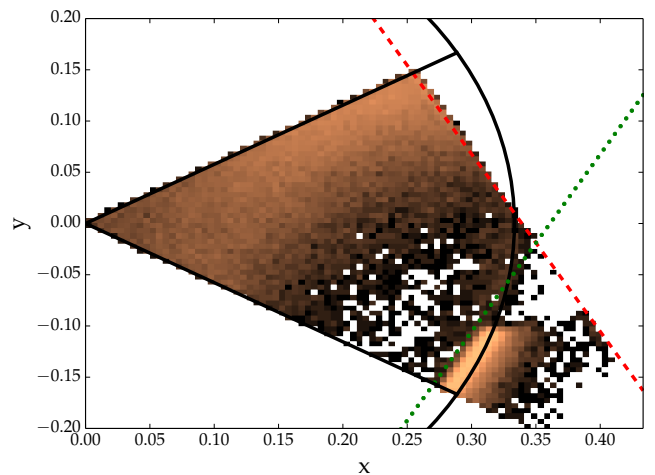


Fig. 7. Dalitz plot of the detected tuples of α particles. The circle indicates the constraints imposed by energy and momentum conservation. The dashed red line indicates the low energy cut off. The dotted green line indicates the distinction between decays via the α_0 (right) and α_1 (left) channels.

in the target. Here α_0 was generated and emitted according to the observed angular distribution in section 3.1. The secondary particles were ejected isotropically according to conservation of angular momentum. These particles were propagated out of the target and into the detectors. Energy loss was taken into account using the SRIM energy loss tables [21]. The output of the simulation had a structure which was identical to the data and was thus subjected to the same analysis. From the survival ratio an acceptance was determined

$$\eta_0 = 7.1(3) \% \quad (9)$$

Correcting for the efficiency gives a cross section of

$$\sigma_{p\alpha,0} = 2.0(2) \text{ mb}, \quad (10)$$

which is consistent with the singles analysis.

3.4 Detection efficiency of the α_1 channel

The detection efficiency depends heavily on the ^8Be excitation energy as it determines the opening angle between the secondary α particles. Laursen *et al.* found that their sequential decay model fully described their data [7]. Thus, events were generated using this model. Propagation and energy loss was done with the same procedure as described in the previous section. From the survival ratio the acceptance was determined to be

$$\eta_1 = 0.49(5) \% \quad (11)$$

This yields a cross section to the excited channel of

$$\sigma_{p\alpha,1} = 38(5) \text{ mb}. \quad (12)$$

4 Discussion

Both values determined for the α_0 cross section are consistent with the measurement by [6]. The weighted cross section is

$$\sigma_{p\alpha,0} = 2.03(14) \text{ mb.} \quad (13)$$

Comparing the angular distribution in Figure 5 with previous measurements, good agreement is observed between our measurement and Ref. [5] while our measurement agrees poorly with Ref. [6]. Most significantly a symmetric behavior around 90° is only observed by Ref. [6]. Additionally, we argue that the error bars of Ref. [5] do not include an overall systematic uncertainty of $\sim 5\%$, which is visible in their repeated measurements at 90° .

Subtracting the α_0 cross section from the α_1 cross section measured by Refs. [4,5] yields 39(3) mb and 52(6) mb respectively. Thus, excellent agreement is observed for the former result and reasonable agreement with the latter. Additionally, the measurement by [6] is roughly a factor 2 larger than observed here. However, rescaling their results by a factor $2/3$ yields 46(3) mb. Considering, [6] reported methodical problems at this energy, this agreement is acceptable. However, their error bars should most likely be increased somewhat. We have chosen a conservative 15%. Combining all measurements the total α resonance cross section is

$$\sigma_{p\alpha} = 43(2) \text{ mb.} \quad (14)$$

The α branching ratio from the measurements of the two cross sections is 18(3), which is consistent both previous measurements. Combining all three measurements

$$\frac{\sigma_{p\alpha,1}}{\sigma_{p\alpha,0}} = 19.9(14). \quad (15)$$

5 Derived partial widths

Using the present measurement of the (p, α) cross section the partial proton width can be determined using Eq. (1)

$$\Gamma_p = 19(3) \text{ eV,} \quad (16)$$

while using the combined cross section yields

$$\Gamma_p = 21.0(13) \text{ eV.} \quad (17)$$

Both of which are consistent, within the errors, with that of the latest evaluation [14], but not with the value favored by [12][12].

Combining this proton width with the results of [13] and Γ , the partial gamma widths can be determined

$$\Gamma_{\gamma 0} = 0.62(8) \text{ eV} \quad (18)$$

$$\Gamma_{\gamma 1} = 17(2) \text{ eV.} \quad (19)$$

These values are consistent with the latest evaluation [14], but inconsistent with a direct measurement using inelastically scattered electrons, which measured $\Gamma_{\gamma 0} = 0.346(41) \text{ eV}$.

While direct measurements should generally be favored, in this case there is multiple independent and consistent measurements of the remaining parameters. In order to resolve this discrepancy we suggest that $\Gamma_{\gamma 0}$ is remeasured in a direct manner.

Combining the improved total α cross section with the γ cross sections measured by [13] the branching ratio can be determined

$$\frac{\Gamma_{\gamma 0}}{\Gamma_\alpha} = 1.18(13) \times 10^{-5} \quad (20)$$

$$\frac{\Gamma_{\gamma 1}}{\Gamma_\alpha} = 3.2(3) \times 10^{-3} \quad (21)$$

which is inconsistent with the measurement by [10]. Considering the general spread of the measured α cross sections, the most likely explanation for this discrepancy is that the α yield have been overestimated.

6 Conclusion

Using the $p + ^{11}\text{B}$ reaction, the break-up of the 16.1 MeV state in ^{12}C into three α particles has been studied using an array of large area segmented silicon detectors in close geometry. The decay via the ground state of ^8Be has been studied both with detection of single particles and coincident detection of all three α particles. The derived cross sections are internally consistent and the combined result is

$$\sigma_{p\alpha,0} = 2.03(14) \text{ mb,} \quad (22)$$

which is consistent with the result of Ref. [6].

Currently, there exists multiple incompatible measurements of the decay via the first excited state of ^8Be . This channel was studied using coincident detection of all three α particles. The coincidence acceptance can be determined using the decay model of Ref. [7] yielding a model dependent cross section

$$\sigma_{p\alpha,1} = 38(5) \text{ mb.} \quad (23)$$

which is, within the errors, consistent with Ref. [4,5] but not Ref. [6].

The inconsistency with Ref. [6] is due to their claim of having a substantial chance of detecting two out of three particles with a single detector. This was discussed based on Ref. [19]. The chance of this is minuscule and hence the entire α_1 dataset of Ref. [6] should be rescaled by a factor $2/3$. If this rescaling is performed it is consistent with all other measurements.

Combining all measurements of $\sigma_{p\alpha}$ a refined partial proton width of $\Gamma_p = 21.0(13) \text{ eV}$ was derived. This in turn, was used to determine the partial gamma widths $\Gamma_{\gamma 0} = 0.62(8) \text{ eV}$ and $\Gamma_{\gamma 1} = 17(2) \text{ eV}$, using the combined γ cross sections measured reported by Refs. [13]. The value for $\Gamma_{\gamma 0}$ differs by roughly a factor of 2 from the direct measurement of Ref. [9]. Hence, we recommend that $\Gamma_{\gamma 0}$ is remeasured.

Additionally, improved γ - α branching ratios are derived. These are roughly a factor of 2 larger than the

measurements published by [10]. We speculate that this discrepancy is most likely due to [10] having overestimated the α yield.

22. M. Alcorta, O. Kirsebom, M. Borge, H. Fynbo, K. Riisager, O. Tengblad, Nuclear Instruments and Methods in Physics Research Section A: Accelerators, Spectrometers, Detectors and Associated Equipment **605**, 318 (2009)

7 Acknowledgement

We would like to thank Folmer Lyckegaard for manufacturing the target. We also acknowledge financial support from the European Research Council under ERC starting grant LOBENA, No. 307447.

References

1. T. Huus, R.B. Day, Phys. Rev. **91**, 599 (1953)
2. O. Beckman, T. Huus, Č. Zupančič, Phys. Rev. **91**, 606 (1953)
3. R.E. Segel, M.J. Bina, Phys. Rev. **124**, 814 (1961)
4. B. Anderson, M. Dwarakanath, J. Schweitzer, A. Nero, Nucl. Phys. A **233**, 286 (1974)
5. J.M. Davidson, H.L. Berg, M.M. Lowry, M.R. Dwarakanath, A.J. Sierk, P. Batay-Csorba, Nucl. Physics, Sect. A **315**, 253 (1979)
6. H.W. Becker, C. Rolfs, H.P. Trautvetter, Zeitschrift für Phys. A At. Nucl. **327**, 341 (1987)
7. K.L. Laursen, H.O.U. Fynbo, O.S. Kirsebom, K.O. Madsbøl, K. Riisager, K.S. Madsbøll, K. Riisager, Eur. Phys. J. A **52**, 271 (2016), [1604.01244](#)
8. E.G. Adelberger, R.E. Marrs, K.A. Snover, J.E. Bussolletti, Phys. Rev. C **15**, 484 (1977)
9. A. Friebel, P. Manakos, A. Richter, E. Spamer, W. Stock, O. Titze, Nucl. Phys. A **294**, 129 (1978)
10. F. Cecil, D. Ferg, H. Liu, J. Scorby, J. McNeil, P. Kunz, Nucl. Phys. A **539**, 75 (1992)
11. S. Stave, M. Ahmed, R. France, S. Henshaw, B. Müller, B. Perdue, R. Prior, M. Spraker, H. Weller, Phys. Lett. B **696**, 26 (2011)
12. K.L. Laursen, H.O.U. Fynbo, O.S. Kirsebom, K.S. Madsbøll, K. Riisager, Eur. Phys. J. A **52**, 370 (2016), [1610.00509](#)
13. J.J. He, B.L. Jia, S.W. Xu, S.Z. Chen, S.B. Ma, S.Q. Hou, J. Hu, L.Y. Zhang, X.Q. Yu, Phys. Rev. C - Nucl. Phys. **93**, 1 (2016)
14. J. Kelley, J. Purcell, C. Sheu, Nuclear Physics A **968**, 71 (2017)
15. C. Labaune, C. Baccou, V. Yahia, C. Neuville, J. Rafelski, W.M. Nevins, R. Swain, H. Hora, A. Picciotto, D. Strickland et al., Sci. Rep. **6**, 21202 (2016)
16. D.S. Craig, W.G. Gross, R.G. Jarvis, Physical Review **103**, 1414 (1956)
17. F. Ajzenberg, T. Lauritsen, Reviews of Modern Physics **24**, 321 (1952)
18. F. Ajzenberg-Selove, Nucl. Phys. A **506**, 1 (1990)
19. J.A. Wheeler, Phys. Rev. **59**, 27 (1941)
20. M. Chiari, L. Giuntini, P. Mandò, N. Taccetti, Nucl. Instruments Methods Phys. Res. Sect. B Beam Interact. with Mater. Atoms **184**, 309 (2001)
21. J.F. Ziegler, M.D. Ziegler, J.P. Biersack, Nuclear Instruments and Methods in Physics Research B **268**, 1818 (2010)